NEUROSCIENCE RESEARCH NOTES

ISSN: 2576-828X

OPEN ACCESS | RESEARCH NOTES

Investigating cortical networks from vibrotactile stimulation in young adults using independent component analysis: an fMRI study

Faten Anis Syairah Seri ¹, Aini Ismafairus Abd Hamid ^{1,2,3}*, Jafri Malin Abdullah ^{1,2,3}, Zamzuri Idris ^{1,2,3}, Hazim Omar ^{1,2,3} and Muhd Riddha Abdul Rahman ^{1,2}

- ¹ Department of Neurosciences, School of Medical Sciences, Universiti Sains Malaysia, 16150 Kubang Kerian, Kelantan Malaysia.
- ² Brain and Behaviour Cluster, School of Medical Sciences, Universiti Sains Malaysia, 16150 Kubang Kerian, Kelantan Malaysia.
- ³ Hospital Universiti Sains Malaysia, 16150 Kubang Kerian, Kelantan, Malaysia.
- * Correspondence: aini ismafairus@usm.my; Tel: +609-7676348/6300

Received: 11 October 2022; Accepted: 26 April 2023; Published: 4 July 2023 Edited by: Kamalanathan Palaniandy (Universiti Kebangsaan Malaysia, Malaysia)

Reviewed by: Subapriya Suppiah (Universiti Putra Malaysia, Malaysia); Ahmad Nazlim Yusoff (Universiti Kebangsaan Malaysia, Malaysia); Indranath Chatterjee (Tongmyong University, South Korea)

https://doi.org/10.31117/neuroscirn.v6i3.194

Abstract: This study investigated the functional connectivity of the neural networks when vibrotactile stimulation is applied to the fingertips of young adults. Twenty healthy, right-handed subjects were stimulated with vibrotactile stimulation whilst being scanned with a 3.0 T magnetic resonance imaging scanner. The subjects were stimulated at 30 Hz - 240 Hz using a piezoelectric vibrator attached to the subjects' bilateral index fingers. The scanned data were processed with independent component analysis (ICA), while the temporal configuration and spatial localisation of the component were investigated. The activation locations were tabulated and compared with regions of somatosensory in the brain. Using ICA, somatosensory regions and their neighbouring areas identified one or more of these components mapped to the common significant regions in the medial frontal gyrus (MFG), paracentral lobule (PaCL), precentral gyrus (PrG), postcentral gyrus (PoG), inferior parietal lobule (IPL), and cingulate gyrus (CgG). Using Neuromark as a reference, six significant networks with the highest correlation values, r>0.5, were identified: the visual network (VIN), sensorimotor network (SMN), cognitive-control network (CCN), subcortical network (SCN), default-mode network (DMN), and auditory network (AUN). It showed that VIN and SMN were the most activated during the vibrotactile stimulation. A comparison of the network volumes and peak activations during the conditions demonstrated changes in volume and corresponding peak activation during vibrotactile stimulation. This study contributes to a better understanding of the underlying mechanisms of the somatosensory areas. Other than that, not only this study highlighted the underlying effect of vibrotactile stimulation towards the functional brain connectivity at network levels, but it also highlighted the impact of frequencies in somatosensory studies. In the future, we suggest that exploring the change in the range of frequencies and examining its differences will allow us to comprehend aspects of somatosensory networks and their connectivity.

Keywords: somatosensory; functional magnetic resonance imaging (fMRI); vibrotactile; functional connectivity; independent component analysis

©2023 by Seri *et al.* for use and distribution in accord with the Creative Commons Attribution (CC BY-NC 4.0) license (https://creativecommons.org/licenses/by-nc/4.0/), which permits unrestricted non-commercial use, distribution, and reproduction in any medium, provided the original author and source are credited.

1.0 INTRODUCTION

The study involving the somatotopic mapping of the somatosensory areas and their neighbouring regions has been a major focus. The primary (S1) and secondary (S2) somatosensory cortices are different in how it connects to prefrontal areas and how it encodes cognitive aspects of tactile processing (Friedrich et al., 2018; Kim et al., 2015; Nazarian et al., 2022). Recent studies using vibrotactile stimuli to examine cognitive processes have proven reliable in eliciting responses from somatosensory areas. The vibrotactile stimuli have been applied to young adults in areas such as bilateral fingertips (Chung et al., 2013; Goltz et al., 2013; Puckett et al., 2017; Seri et al., 2019, 2020), digits fingertips (Francis et al., 2000; Pfannmöller et al., 2016; Schweisfurth et al., 2011, 2014, 2015), right forearms (Malone et al., 2019), breast (Beugels et al., 2020), leg and foot (Akselrod et al., 2017), sole of the right foot (Siedentopf et al., 2008), and the chest, chin and arm (Jung et al., 2018). Similarly, it was observed that the vibrotactile stimulation using a piezoelectric stimulation system shows good congruency in the S1 cortex using fMRI (functional magnetic resonance imaging) response location (Jaatela et al., 2022), thus proving the reliability of vibrotactile as a stimulus to evoke responses in the somatosensory areas.

Previous studies have mentioned the effect of vibrotactile stimulation that involves low frequencies that mostly activated the S1 areas, such as a study using the frequency of 3 Hz (Pfannmöller et al., 2016) and that involved high frequencies that have activated S1 and S2 areas, such as a study using the frequency of 250 Hz (Choi et al., 2016). Previous literature also mentioned that integrating the low and high frequencies yields significant responses in the somatosensory areas and their neighbouring regions, including the S1 and S2 (Chung et al., 2013; Wu et al., 2021). However, few studies have been conducted to investigate the functional connectivity of the region involved in activation due to vibrotactile stimulation of somatosensory areas at varying frequencies.

Functional connectivity is defined as the temporal coincidence of spatially distant neurophysiology events (<u>Eickhoff & Müller, 2015</u>), with two regions said to have functional connectivity if there is a statistical relationship between measures of activity recorded for them. Independent component analysis (ICA) is a blind-

sourced separation method (Moritz et al., 2000) widely used to estimate functional brain networks from fMRI data (Du et al., 2021; Zhao et al., 2021). As an effective data-driven method, when the research paradigm does not include any prior knowledge that denotes its physiology meaning without time course, ICA is more likely preferred compared to the model-driven methods like General Linear Model (GLM) or Dynamic Causal Modelling (DCM) method (Zhao et al., 2021) during MRI studies. In principle, ICA identifies the haemodynamic responses regardless of the interval, duration, or magnitude within the data (Moritz et al., 2000). As the study insisted on understanding the interaction at a network level, examining the significant region at the network level was suggested to contribute to a broader understanding of human cognition (Rabe et al., 2021).

Additionally, the neural interaction among the multiple activated regions or cognitive domains is expected and it plays a role in task information processing. It was proposed that most (~78%) functional brain regions showed an overlap of two or more functional networks (FNs) (Xu et al., 2013). Multiple overlaps of neural circuits with unique time-course and task modulation occurrences in the same voxel or region were not detected by GLM-based analysis. Thus, functional connectivity analysis using ICA as a signal processing technique that utilises higher order statistics to extract signals by unmixing signals mixture (Xu et al., 2013) are proven to be a promising method for investigating the intrinsic neuronal activity in task-based studies (Wu et al., 2018).

This study aims to examine the functional connectivity of the neural networks when vibrotactile stimulation was performed on the fingertips of young adults by using the state-of-the-art data-driven method called ICA. Using ICA, the temporal characteristics and the spatial mapping of extensive networks identified by ICA will further enhance our apprehension regarding how the stimulus of vibrotactile affects the temporal mapping of the brain and how the neural networks responded to the varying stimulus of vibrotactile frequencies. This study will further enhance the understanding of the underlying mechanisms of vibrotactile stimulation. It is significantly useful as a fundamental study to review the effect of vibrotactile stimulation and its impact on the cortical areas. Ultimately, the study might provide promising

neuroimaging-based outcomes that will be useful, particularly in an intervention study.

2.0 MATERIALS AND METHODS

2.1 Experimental paradigm

A total of 20 subjects have undergone fMRI scanning from May 2018 until August 2020. Twenty healthy righthanded subjects (n=20, 14 males and 6 females, aged 20 ± 10 years, mean=25.1, SD=5.01) with no neurological or psychiatric diseases were scanned with a 3.0 T MRI scanner (Achieva, Philips, Netherlands) equipped with a 32-channel SENSE head coil. The experimental procedures were conducted per the principles of the Declaration of Helsinki (World Medical Association, 2013), and approval of the protocol was obtained from the Human Research Ethics Committee of USM (HREC) (USM/JEPeM/17070349). A block design paradigm of low and high frequency in this study as described by Seri et al. (2019, 2020), was developed using E-Prime 1.0 software (Psychology Software Tools, Pittsburgh, PA) to synchronise the timing with the MRI scanner. All participants were right-handed, as measured by Edinburgh Handedness Inventory (Oldfield, 1971). Each participant wore an eye mask to reduce visual artefacts in the MRI room (Golaszewski et al., 2002). Additionally, the noise from the 3.0 T MRI scanner can be uncomfortably loud as the exposure to such noise levels can create discomfort to the subjects (Motovilova & Winkler, 2022). According to Motovilova and Winkler (2022), exposure to acoustic noise due to a 3T scanner may manifest as motion artefacts and degraded the image quality. Thus, each participant wore earplugs and headphones to reduce the acoustic noise produced by the scanner. Additionally, the subjects' head was immobilised using foam paddings to minimise movement artefacts (Francis et al., 2000). To ensure the image quality, image analysis was performed using MATLAB R2020a (Mathworks Inc., Natick, MA, USA) and the Statistical Parametric Mapping 12 (Wellcome Department of Imaging Neurosciences, Institute of Neurology, University College of London, UK) software packages. The data analysis involved the following preprocessing steps: 1) slice-timing, 2) realignment, 3) normalisation, and 4) smoothing (full-width half maximum of 6 mm), where the activated brain regions were identified with Wake Forest University (WFU) PickAtlas software. Further details on the paradigm design were described in Seri et al. (2019, 2020).

2.2 The MR image acquisition

The vibratory stimulus was delivered using an MRI-compatible piezoelectric finger stimulation system device (Ben Krasnow, Redwood City, CA). The

piezoelectric actuators were attached to the subject's left, and right index fingertips, and the vibration was produced through the transmission of an alternating current. The stimulation frequencies range from 30 Hz to 480 Hz. The neuroimaging data were obtained using a 3.0 T MRI scanner (Achieva, Philips, Netherlands) equipped with a 32-channel SENSE head coil. For anatomical localisation process, each subject produced the T1-weighted, high-resolution structural image (TR/TE/slice/FOV = 9.7ms/4.6ms/1.2mm/250mm x 250mm). An echo-planar imaging (EPI) sequence with the following parameter (TR/TE/slice/flip angle/FOV = 3000ms/33ms/4mm slices/80°/230mm) was also applied for the acquisition process.

2.3 The fMRI independent component analysis (ICA)

In this study, the ICA processing was performed using a pipeline called Neuromark, as described in Du et al. (2020). The pre-processed time series were analysed using the Group ICA of fMRI Toolbox (GIFT, https://trendscenter.org/software/gift/, version 3.0c) to identify spatially independent and temporally coherent networks. A low model order of group-level spatial ICA was applied to obtain large-scale networks representing brain network module (Elseoud et al., 2011). For group ICA, according to the minimum description length (MDL) criterion, the optimal number for group ICA was 20 components (Rosazza et al., 2012). According to Rosazza et al. (2012), MDL is described as an information-theoretic criterion that corresponds to choosing the model, permitting the most compact encoding of the data and the model itself. As cited in Rosazza et al. (2012), this criterion is the most frequently adopted in determining the optimal number of ICA components for a given dataset.

Variance normalisation (z-score) was applied on voxel time courses and computed subject-level spatial principal component analysis (PCA) to retain maximum subject-level variance (greater than 99%). Subject-level principal components were concatenated together across time dimensions, and group-level spatial PCA was applied to the concatenated subject-level principal components. The 20 group-level principal components that explained the maximum variance were selected as the input for the Infomax algorithm to calculate 20 group-independent components. To minimise the impacts of artefacts, we first ran ICA on each subject individually. After inspecting all images on the individual subject level, cleaned images of all 20 subjects were included in group ICA. The method is detailed in the following sections:

(A) Single subject analysis

Independent component (IC) estimation was performed using the Infomax algorithm, which was repeated 25 times regularly to maximise the stability of the derived components. The dimensionality of the data (the number of networks) was estimated per subject using the MDL criteria tool built into GIFT. Images were back-reconstructed using GICA3, a back-reconstruction method in which individual subject maps are reconstructed from the raw data using the ICA mixing matrix. Time series were converted for visualisation to reflect percent signal change. After single subject ICA, both spatial pattern and the frequency spectrum of each component were inspected for possible image artefacts. Components containing obvious artefacts (e.g., edges, ventricles) were discarded.

(B) Group analysis

The cleaned data were carried forward to group analysis. Group ICA was performed using the Infomax algorithm, repeated 25 times with regular stability analysis. The number of components estimated through MDL was 44. Individual subject component maps were back-reconstructed using GICA, and finally, time courses and spatial maps were normalised into z-scores.

(C) Identifying reliable, functional network templates We performed ICA on the dataset to yield reliable ICs. First, the principal component analysis (PCA) was performed on each subject to reduce fMRI data to 25 principles components (PCs). Then, the individual-level PCs of each subject were concatenated across different subjects. Next, the Infomax algorithm was applied to decompose the 25 PCs into 25 ICs (Du & Fan, 2013). This procedure was repeated 20 times using the ICASSO technique, where the best ICA run was selected to generate 25 reliable IC (Du & Fan, 2013).

(D) Selection of networks

In selecting significant neuronal networks in this study, the correspondence of components across subjects was used as the basis for meaningful comparisons. Thus, to find a reproducible network in this study, two statistical analyses of spatial correlation were applied to understand the relationship between the networks and the vibrotactile stimulation. The two statistical analyses are the Pearson correlation and Spearman correlation. The Pearson correlation was applied to measure the correlation value of the spatial coefficient (Boslaugh & Watters, 2008) during vibrotactile stimulation. Meanwhile, the Spearman correlation was used to measure the degree of association (Ali & Al-Hameed, 2022) of the networks during vibrotactile stimulation.

Thus, the Cohen's Standard was used as a reference to determine the strength of the association during vibrotactile stimulation and the effect size of the correspondence ICs. According to Cohen's Standard, correlation coefficients between 0.10 and 0.29 represent a small association, coefficients between 0.30 and 0.49 represent a medium association, and coefficients of 0.50 and above represent a large association or relationship (Quintana, 2023). As a result, it was found that the value of the degree of association of the vibrotactile stimulation with spatial correlation for the 25 ICs was (r=0.39, P<0.001). Using the correlation coefficient metrics, 17 ICs from the 25 ICs were discarded. This is because the components discarded showed a high spatial correlation with the probabilistic map of white matter or cerebrospinal fluid provided in SPM12, while showing low correlations with the cerebral grey matter map. Using visual inspection, the 17 discarded ICs suggested that the high spatial correlation was associated with eye movements, head motion, or cardiac-induced pulsatile artefacts at the base of the brain. Thus, to compute the degree of taskrelatedness of the remaining 8 ICs components, we regressed the corresponding time courses against the design matrix using the temporal multiple linear regression implemented in the GIFT. The remaining 8 ICs were selected for the final analyses, with correlations significant at p<0.001 with vibratory stimulation of various frequencies. They were named according to the template they were spatially correlated with or based on the visual inspection of the corresponding spatial map.

3.0 RESULTS

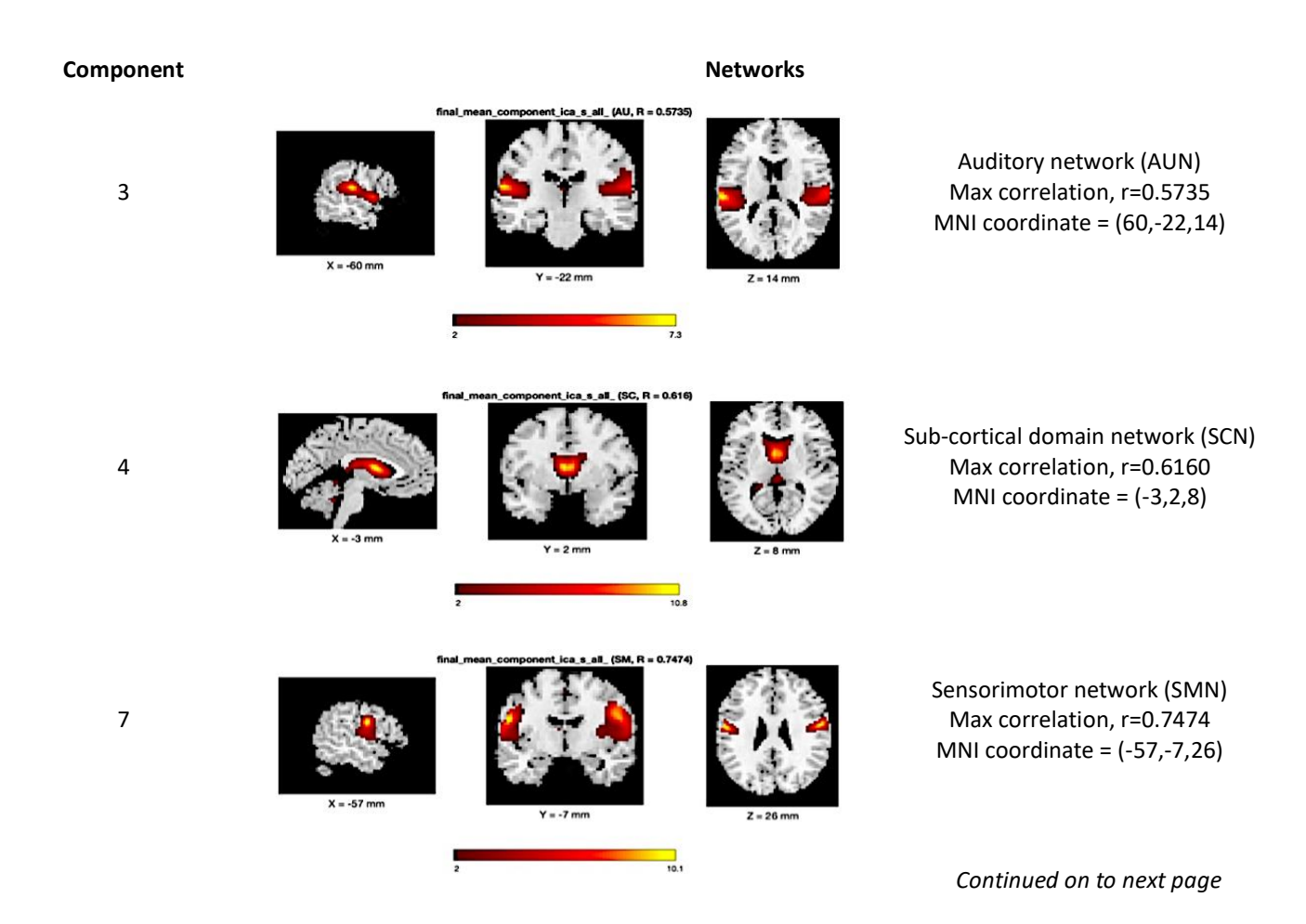
3.1 Connectivity analysis - Independent Component Analysis (ICA)

Figure 1 displays the eight networks with components with significant correlation (r>0.5). To examine the components, the spatial association of the components during vibrotactile stimulation was determined using Spearman analysis. Using Spearman, a correlation value (r=0.39, P<0.001) was generated. It highlighted the degree of association of the components during the vibrotactile stimulation (Ali & Al-Hameed, 2022). Using Cohen's standard as a reference, it was determined that the association was categorised as a medium association (Quintana, 2023). This reflected the spatial coefficients of the 25 components during the vibrotactile stimulation. In selecting the significant networks during the vibrotactile stimulation, Pearson correlation was applied to examine networks with high correlation values. The Pearson correlation was applied to investigate the strength of the relationship of the components and their effect size during the vibrotactile

stimulation (<u>Boslaugh & Watters</u>, <u>2008</u>). Using Pearson correlation, it was found that the 25 components generated a correlation value of (r=0.44, P<0.001), signifying the medium strength of the significant components with the vibrotactile stimulation.

A pipeline known as Neuromark was utilised to automate the estimation of the subject-specific functional network with associated time courses (TCs) (Du & Fan, 2013). Additionally, Neuromark was used as a reference in labelling individual-subject connectivity features, which incorporated an additional input of the spatial network (Du et al., 2020). To examine the spatial correspondence of the ICs, whole-brain voxels were taken as input for the Neuromark template. Using Neuromark as a reference, the spatial correlation matrices reflected the similarity between the matched two groups of functional networks or components, which also reflected the spatial correspondence of the ICs (Du & Fan, 2013). Using Pearson correlation, the 8 locations of the components were tabulated in Figure 1. By exploring the spatial correlation matrices, the location of the components was compared with the locations of the regions involved in the organisation of somatosensory and its neighbouring regions in the brain. The spatial maps of the somatosensory networks

compared with the components were depicted in a circle illustrated in Figure 2(b). By means of ICA, there were 6 components with a correlation value of medium association according to Cohen's standard. By exploring the spatial correlation matrices and comparing them to the somatosensory regions, it was found that 6 networks reflected significant correlation during vibrotactile stimulation. The dominant network, according to the correlation value (r>0.5, p<0.001), was the visual network (VIN), sensorimotor network (SMN), sub-cortical network (SCN), cognitive-control network (CCN), auditory network (AUN), and default-mode network (DMN). Across all subjects, common significant regions were activated in all components, with reference to Neuromark template. The common activated regions were tabulated in Table 1. Meanwhile, **Table 2** tabulated the activated brain areas across the network that was captured by the 25 components. Figure 2 depicts the connectogram view of functional network connectivity (FNC) correlations. Figure 2(a) depicts the strength of connections of the components in the same network. The components of the same networks were shown in the same colour. It tabulated the amount of the components in the same network involved in the vibrotactile stimulation.



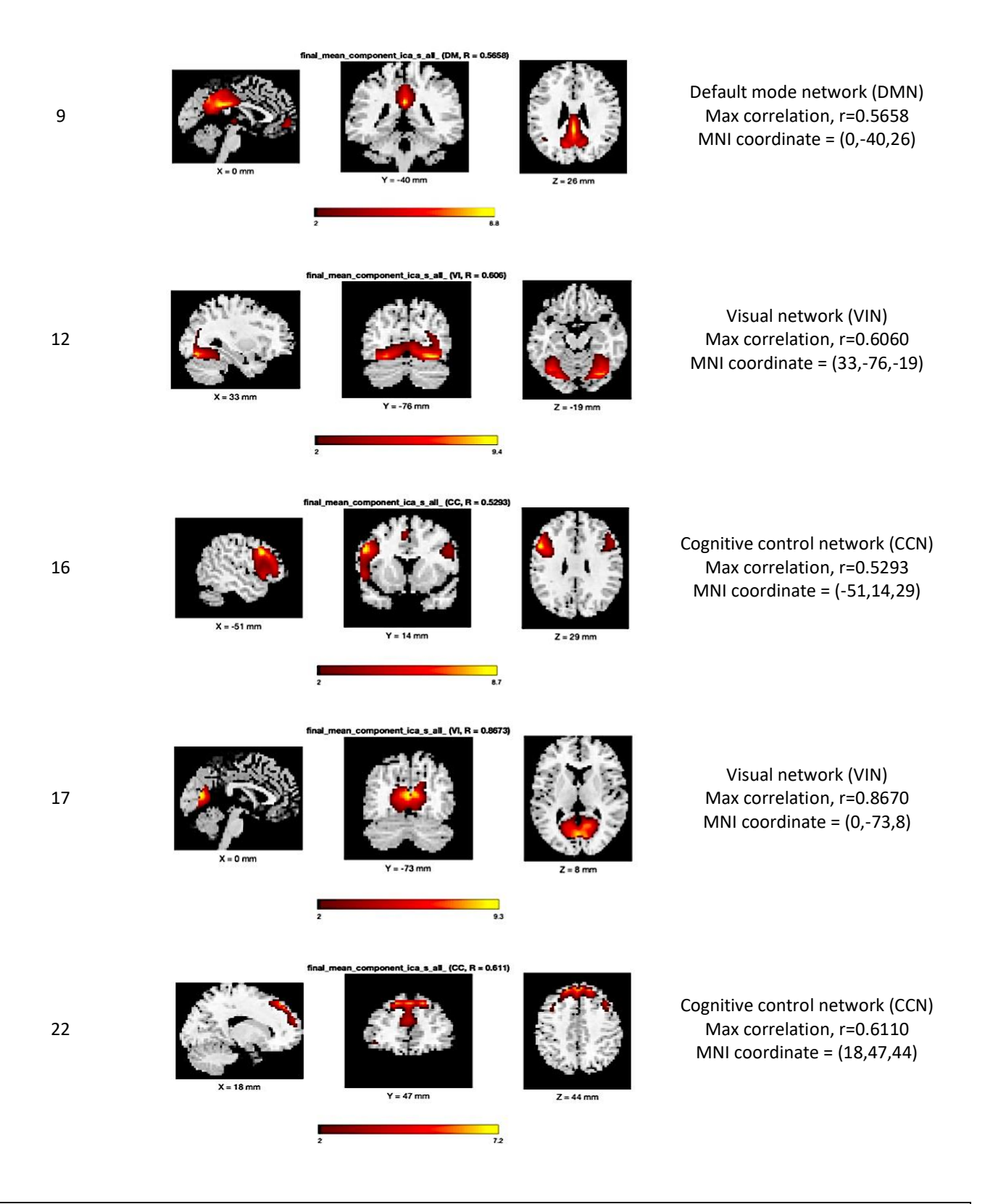


Figure 1: Spatial maps for the 8 ICs of the 25-ICs decompositions, each viewed in three orthogonal directions. The MNI coordinates refer to the slice intersections that are shown. The group-level t-maps are thresholded at t>1.96 and the templates follow Neuromark.

Table 1: The significant common areas in all IC across all subjects and sessions where the component labelling follows Neuromark.

Areas	BA	Vol. (cc)	MNI coordinate [x, y, z]	
Medial frontal gyrus	6, 32	2.0/2.1	[0, -19, 54]	
Paracentral lobule	5, 6, 31	2.6/2.5	[0, -28, 54]	
Precentral gyrus	3, 4, 6	0.6/2.1	[-2.85, -28, 54]	
Postcentral gyrus	2, 3, 40, 43	1.3/5.2	[-33, -2.65, 50]	
Inferior parietal lobule	40	0.6/1.5	[-4.35, -3.25, 42]	
Cingulate gyrus	24, 31, 32	3.6/3.5	[-33, -2.65, 50]	

Abbreviations: BA=Brodmann Area, Vol=volume

Table 2: The components covering the listed networks also included other brain areas that are not typically listed in these networks shown below, where the component labelling follows Neuromark.

Comp.	Areas	ВА	Vol. (cc)	MNI [x, y, z]
IC3	Transverse temporal gyrus	41, 42	1.5/1.3	[-5.55, -2.35, 10]
	Superior temporal gyrus	13, 22, 38, 41, 42	7.3/6.5	[-63, -2.65, 14]
	Insula	13, 22, 40	3.1/3.2	[-51, -2.35, 14]
IC4	Lateral ventricle	-	4.9/4.2	[-3, 3.5, 10]
	Caudate	-	3.0/3.3	[-7.5, 6.5, 10]
	Thalamus	-	1.2/1.3	[-6, -4, 10]
IC7	Superior temporal gyrus	22	2.0/1.7	[-6.15, -4, 10]
	Transverse temporal gyrus	41, 42	0.8/0.4	[-6.15, -8.5 14]
	Insula	13	1.2/1.7	[-3.75, -13, 14]
IC9	Precuneus	7, 23, 31	4.8/4.9	[0, -5.95, 34]
	Posterior cingulate	23, 29, 30, 31	2.8/2.5	[0, -5.35, 18]
	Paracentral lobule	5, 31	0.5/0.4	[0, -4.45, 50]
IC12	Fusiform gyrus	19, 20, 37	2.8/3.2	[-2.55, -7.75, -18]
	Lingual gyrus	18, 19	4.0/5.0	[-24, -7.45, -14]
	Middle occipital gyrus	19, 37	0.9/2.0	[-3.45, -7.75, -14]
	Sub-gyral	37	2.4/4.0	[-4.05, -6.85, -14]
1C16	Inferior frontal gyrus	9, 10, 44, 45, 46, 47	13.4/2.3	[-4.95, 1.25, 30]
	Sub-gyral	40	3.3/0.7	[-42, 14, 26]
	Superior frontal gyrus	6, 8	1.2/0.1	[-1.5, 1.25, 54]
	Superior temporal gyrus	22, 38	0.7/0.0	[-5.25, 9.5, 2]
1C17	Cuneus	7, 17, 18, 23, 30	2.4/2.4	[-4.5, -73, 10]
	Posterior cingulate	23, 29, 30, 31	2.8/3.4	[-3, -6.85, 10]
	Lingual gyrus	18, 19	5.0/4.3	[-12, -5.65, 2]
	Precuneus	7, 23, 31	1.2/1.8	[(0, -7.15, 18]
1C22	Superior frontal gyrus	8, 9, 10	7.6/8.1	[-1.5, 4.25, 50]
	Inferior frontal gyrus	47	1.1/0.8	[-48, 2.15, -6)

Abbreviations: Comp=component, BA=Brodmann Area, Vol=volume

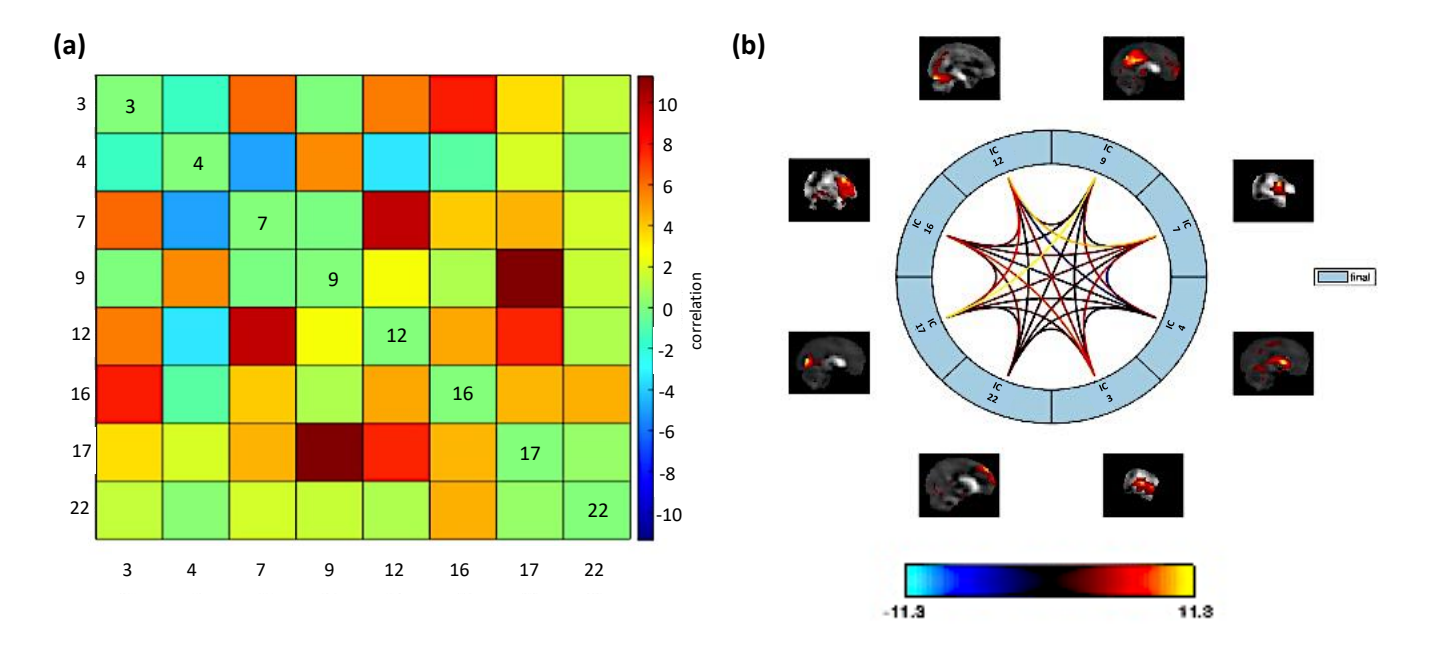


Figure 2: Connectogram view of functional network connectivity (FNC) correlations. **(a)** The figure of Bezier curves that shows components of the same network having the same colour; **(b)** thumbnails of spatial maps are presented in a circle.

4.0 DISCUSSION

4.1 Common regions during vibrotactile stimulation

This study activated a few common significant regions during the vibrotactile stimulation. As in previous literature, the regions activated were known due to its somatotopic mapping being in the S1 and S2 area. The vibrotactile stimulation elicited significant activation in the medial frontal gyrus (MFG), paracentral lobule (PaCL), precentral gyrus (PrG), postcentral gyrus (PoG), inferior parietal lobule (IPL), and cingulate gyrus (CgG). The activation in the MFG was discovered to be one of the most common significant regions activated during vibrotactile stimulation, and the region is active during a variety range of cognitive operations (Sung et al., 2007). The associative region is the frontal region (Rabe et al., 2021).

Meanwhile, activation of the PaCL is due to its anatomical structure. The region represented the lower limb in the S1 area (Pechenkova et al., 2019), and the anatomical structure of S1 includes the PoG, central sulcus (cis), postcentral sulcus (pcs), and PaCL (Willoughby et al., 2021). Furthermore, the region has been shown to produce significant activity during light tactile stimulation (Hagen & Pardo, 2002). Meanwhile, activation in the PrG (Rabe et al., 2021) and PoG (Malone et al., 2019) are common during vibrotactile stimulation. The activation was suggested to be caused by the overlapping activity in the precentral, postcentral, and premotor cortices during vibrotactile stimulation (Cassady et al., 2020). The PrG that covers the locus of

the primary motor cortex (Francis et al., 2000), is responsible for vibrotactile frequency processing and discrimination (Hegner et al., 2007). Hegner et al. (2007) reported that the tactile information in PrG is sensitive to changes in vibrotactile frequency, indicating the manifestation of a significant response adaptation effect during the flow of tactile information from early sensory areas to higher cognitive areas.

Meanwhile, the PoG region is known to carry frequencydependent information in the S1 (Hegner et al., 2010) and S2 areas (Kim et al., 2016). The PoG region was said to be involved in pattern and frequency discrimination. Additionally, Hegner et al. (2007) mentioned that tactile working memory often resides in a network of brain regions, such as in the somatosensory and parietal areas. Recent studies have shown significant differences in brain activation when vibrotactile stimulation of low frequencies and high frequencies is applied. Based on the previous research, it was found that vibrotactile stimulation of low frequencies activated the primary somatosensory regions (Seri et al., 2019), meanwhile stimulation of high frequencies predominantly activated the secondary somatosensory regions (Seri et al., 2020). It was suggested that the activation in the inferior parietal (IPL) in the primary somatosensory area (Seri et al., 2019) was due to the region being evoked during low-frequency vibrotactile stimulation, as opposed to high frequency stimulation (Cole et al., 2022). It was due to the region being a multimodal association area that connects perception and action, acting as an interface between sensory areas and motor planning areas by matching the information generated (Araneda et al., 2021). Vibrotactile stimulation yields bilateral activation of S1 and S2 and the region in the CgG (Beugels et al., 2020). According to the findings of a recent study, the CgG carried frequency-specific information during the tactile study (Uluç et al., 2018). Because the region is part of an overlapping frontoparietal network, it was suggested that it was involved in detecting visual and tactile frequencies (Uluç et al., 2018).

4.2 Association of vibrotactile stimulation with neural networks

The result of the study revealed an association between vibrotactile stimulation and distributed networks, which is consistent with previous vibrotactile research (Sörös et al., 2007). The evaluation performed on the components across subjects using Pearson correlation to measure the strength of a relationship between spatial coefficient with vibrotactile stimulation has generated a correlation value of (r=0.44, P<0.001). According to Cohen's standard, the spatial coefficient with vibrotactile stimulation has generated a medium association. The Spearman correlation was applied to understand and examine the degree of association of vibrotactile stimulation with spatial correlation for the 25 ICs. Thus, with reference to the Cohen's standard, it was found that out of 25 ICs, there were 8 ICs components that correlate highly with the vibrotactile stimulation. The result from the ICA has identified a series of spatially IC. The results show that 1) IC17, VIN has the highest correlation values, r=0.87, followed by 2) IC7, SMN with correlation values, r=0.74, 3) IC4, SCN with correlation values, r=0.62, 4) IC22, CCN with correlation values, r=0.61, 5) IC12, VIN with correlation values, r=0.60, 6) IC9, DMN with correlation values, r=0.57, 7) IC3, AUN with correlation values, r=0.57, and 8) IC16, CCN with correlation values, r=0.53. The results indicated that all eight ICs with r>0.5 were positively correlated per Cohen's criteria (Rosazza et al., 2012) to the vibrotactile stimulation. The VIN in the component IC17 (r= 0.87) and IC12 (r=0.6) were identified as having the highest correlation values. Significant brain activity was detected in the cuneus (Cu), posterior cingulate cortex (PCC), lingual gyrus (LgG), parahippocampal gyrus (PHG), fusiform gyrus (FuG) and middle occipital gyrus (MOG) by IC17 and IC12. A positive correlation was shown in VIN and vibrotactile stimulation. It was proposed that the positive correlation between the VIN and the vibrotactile stimulation was due to the cognitive demand of the given task (Burton et al., 2008). In this study, during the scanning, the subjects' eyes were covered with an eye mask. As the author suggested,

tactile attention tasks involving the cognitive selection of a vibration attribute, such as frequency or duration produced signals that have similar results as visual attention studies. Consequently, significant activation of occipital areas in the Cu, LgG, and MOG was due to the significant role of the occipital cortex in perceiving tactile inputs (Burton et al., 2012). The author found a reduction of response in the occipital region during repetitive learning in blind subjects reflected the role of the occipital region in processing perceptual vibrotactile sequences (Burton et al., 2012). Similarly, the crossmodal recruitment of the occipital cortex during auditory, tactile, and olfactory processing was discovered in a study involving adults with early visual deprivation (Araneda et al., 2021). Thus, tactile input processing with covered visuals helps in memory consolidation, retrieval, or discrimination of the vibrotactile temporal patterns, as Burton et al. (2012) suggested. Activation of the temporal region in the parahippocampal gyrus and FuG is due to the regions being multisensory regions that respond to tactile, auditory, and visual stimulation (Burton et al., 2008). The activation in the caudal region precisely in the PCC is attributed to an event of motor imagery (Sauvage et al., 2011). It was suggested that the involvement of the caudal region is dependent on the complexity of mentally performed movement. The execution and imagination of the same movement activated the same neural network, leading to a hypothesis that motor imagery and motor execution share a similar underlying mechanism (Sauvage et al., 2011).

The IC7 in the SMN detected significant brain activity in the PoG, PrG, superior temporal gyrus (STG), and insula. IC7 has recorded the second-highest correlation values (r=0.74). When responding to vibrotactile stimulation, the S1 area processes tactile information and is significantly activated (Burton et al., 2008). Thus, increased brain activity in the PoG and PrG reflected the somatotopic organisation (Deuchert et al., 2002), explaining the positive correlation with the vibrotactile stimulation as shown in this study. Moreover, activation in the PrG was due to the nature of the motor activation, and the activation expanded to several gyri causing the region to be activated (Maldjian et al., 2003). Meanwhile, activation in the STG was caused by a cortical network of vibrotactile frequency discrimination in humans (Hegner et al., 2007). The STG region has been assumed to function as a sensory polymodal integration area and to be the area where audio-tactile interaction occurred, possibly due to MRI noise (Hegner et al., 2007). Additionally, activation in the insula was caused by a cortical network of vibrotactile frequency

discrimination in humans (<u>Hegner et al., 2007</u>) and multisensory integration centres (<u>Renier et al., 2009</u>).

According to the findings, IC16 and IC22 were identified as CCN, with significant brain activation detected in the PoG, MFG, inferior frontal gyrus (IFG), and superior frontal gyrus (SFG). Increased neural activity in the cortical region of CCN during sensory processing is due to the CCN's high degree of integration, which extends its connectivity with primary sensory and motor cortices (Tomasi & Volkow, 2011). Apart from its importance in sensory processing, the postcentral hub is known to be functionally connected to the SMN, which is one of the major cortical hubs linked to the four cortical networks, which are the DMN, the dorsal-attention network, VIN, and SMN (Tomasi & Volkow, 2011). Furthermore, it was discovered that vibrotactile stimulation activated most of the frontal cortex areas in the MFG, IFG, and SFG. Activation of these areas reflected the goal-directed behaviour when identifying the stimulation target (Burton et al., 2008). According to the author, visual studies involve a dorsal parietal-frontal network, which frequently activates the region involved in goal-directed processes, such as those seen in tactile attention studies (Burton et al., 2008). Apart from that, activation of the S1 area, as seen in the PoG, is consistent with the idea that the S1 region drives and works closely with higher cortical areas, such as frontal areas, to perform sensory discrimination tasks (Hegner et al., 2007).

The IC4 corresponded to the SCN, with significant brain activation detected in the thalamus, caudate and lateral ventricle. A positive correlation was discovered between SCN and vibrotactile stimulation. It was proposed that the positive correlation between the subcortical network and the vibrotactile stimulation was caused by sensory activities (Cerliani et al., 2015). According to the author, this is due to the functionality of the network in processing sensory stimuli, indicating its role in sensoryperceptual processing and discrimination. Apart from that, increased recruitment of cortical and subcortical activity during the early learning phase is thought to be due to the expansion of cortical territory during the early phase of motor learning (Park et al., 2010). The increased activation, according to the author, indicated an improvement in somatosensory feedback. Aside from using vibrotactile stimulation to produce activation in S1 and S2 areas, significant activation in the thalamus was discovered, reflecting its role in sensory information processing (Chakravarty et al., 2009). Furthermore, the response activated in the caudate indicated the subcortical network involvement in processing the vibrotactile stimuli (Golaszewski et al., 2006).

The result obtained showed that IC9 in the DMN, with a significant brain activation detected in the precuneus (PreC), PCC, and PaCL. It was suggested that the positive correlation of DMN with vibrotactile stimulation was due to the widespread activation of a neuronal network that is consistently activated during rest or less demanding tasks (Sörös et al., 2007). Consequently, task-induced reductions in BOLD signals have been observed in the DMN, suggesting increased attentional demands or levels of cognitive engagement (Sengupta et al., 2019). Moreover, the author suggested that the PreC and posterior cingulate activation was attributed to vibrotactile frequency discrimination. activation of the DMN might reflect the generation of spontaneous and internal awareness during vibrotactile stimulation (Tomasi & Volkow, 2011). Moreover, apart from being associated with the DMN activity, the functional connectivity of the PreC that serves as information coding is more associated with active tasks (Woolgar & Zopf, 2017).

Similarly, activity in the DMN area during the active task is reported in the working-memory maintenance study (Sormaz et al., 2018). As reported by the author, the activation is caused by the region being close to the unimodal sensorimotor cortex that serves as a perception and action processing region. Moreover, activation of the PCC, a region located in the DMN area, is due to the region being in a typical motor cortex network of the primary motor area, M1 (Corbetta et al., 2002). Additionally, activation of PaCL reflected the region as a typical motor area to the widespread stimulation (landolo et al., 2018). The result obtained shows that IC3 were identified as AUN, with significant brain activations detected in the STG and insula. The activation of AUN was proposed to be caused by the aversive nature of the background acoustic noise that 'dampens' the sensory processes and hence induces a reduction in the activity related to sensorimotor processing (Rondinoni et al., 2013). In this study, the varying frequencies applied to the vibratory task ranged from 30 Hz to 480 Hz. Generally, auditory data was obtained during airborne low-frequency sound below 200 Hz and infrasound below 20 Hz to be processed in the human central auditory system (Behler & Uppenkamp, 2020). Hence, it was suggested that the positive correlation of the AUN with the vibrotactile stimulation was due to the ability of the AUN to process the auditory information during vibratory stimulation (Cerliani et al., 2015). Regardless of being covered with ear plugs, it was suggested that not only can auditory deprivation enhance the regional activity of STG, but it can also strengthen the spontaneous functional

organisation of the STG network, which also contributed to the cross-modal involvement of the region (<u>Ding et al., 2016</u>).

4.3 Inter-relation between IC components in processing and perceiving the vibrotactile stimulation

Based on a previous study, vibrotactile stimulation typically involves a widespread parieto-fronto-insular network (Rabe et al., 2021). The activity in the SMN and CCN are significantly associated with the vibrotactile stimulation of the fingertips, followed by VIN, DMN, SCN and AUN. SMN and VIN appeared to be important causal hubs for the task and play a critical modulatory role in vibrotactile stimulation. There is also evidence for significant activations in the neighbouring network areas involved, such as DMN, CCN, and AUN, in which the networks are primarily involved in top-down control, implying that they are engaged in primary and secondary processing. As a result, task execution involving vibrotactile stimulation of varying frequencies will activate more brain networks, and the execution of the process will involve greater collaboration among networks.

5.0 CONCLUSIONS

The study seeks to examine the functional connectivity of the neural networks during vibrotactile stimulation using the state-of-the-art data-driven method called ICA. The brain networks involved with somatosensory processing during the stimulation were identified in this study. Understanding how the brain network responds to vibrotactile stimulation is a step forward. There is evidence that the distribution networks are organised in a fashion that suggests the existence of hubs of activity within specific circuits that might influence other neural functions in a manner that directly or indirectly. Thus,

this would enable future studies to understand the functionality and strength of connectivity of the network. It is also suggested that measuring the neural connectivity at different hierarchical levels using ICA might provide an advantage in modelling the systematic effects of pathology in brain disorders for future studies. Moreover, since this study uses healthy participants as the target group, this study can be used as a foundation to compare the effect of the stimulation when incorporating non-healthy subjects such as patients with brain disorders. The results obtained from such studies will be useful to investigate the effect of the stimulation on the brain network and how it affects brain disorders, which in turn helps guide a neurosurgeon in preserving intact brain tissue that, if disrupted, could perhaps induce new clinical impairments or hinder good recovery and helps future researchers further explore brain connectivity, particularly those related to somatosensory.

Acknowledgements: This research was supported by the Universiti Sains Malaysia Short Term Grant: 304/PPSP/6315090. The authors would like to thank the radiographers, Mr. Khew Kuan Kooi, Ms. Che Munirah Che Abdullah, Ms. Siti Afidah Hamat, and Ms. Wan Nazyrah Abdul Halim from the Department of Radiology, Hospital Universiti Sains Malaysia, and Science Officers, Ms. Alwani Liyana Ahmad from the Department of Neurosciences, School of Medical Sciences, Universiti Sains Malaysia.

Author Contributions: F.A.S.S. and A.I.A.H. conceived and designed the study; F.A.S.S., A.I.A.H and H.O. collected the data; F.A.S.S., A.I.A.H and M.R.A.R. analysed the data; F.A.S.S., A.I.A.H wrote the paper; A.I.A.H., J.M., Z.I., H.O. and M.R.A.R. reviewed and edited the paper.

Conflicts of Interest: The authors declare no conflict of interest.

References

Akselrod, M., Martuzzi, R., Serino, A., van der Zwaag, W., Gassert, R., & Blanke, O. (2017). Anatomical and functional properties of the foot and leg representation in areas 3b, 1 and 2 of primary somatosensory cortex in humans: A 7T fMRI study. *NeuroImage*, 159, 473–487. https://doi.org/10.1016/j.neuroimage.2017.06.021

Ali, K., & Al-Hameed, A. (2022). Spearman's correlation coefficient in statistical analysis. *International Journal of Nonlinear Analysis and Applications*, 13, 2008–6822. https://doi.org/10.22075/ijnaa.2022.6079

Araneda, R., Moura, S. S., Dricot, L., & De Volder, A. G. (2021). Beat detection recruits the visual cortex in early blind subjects. *Life*, *11*(4), 296. https://doi.org/10.3390/life11040296

Behler, O., & Uppenkamp, S. (2020). Activation in human auditory cortex in relation to the loudness and unpleasantness of low-frequency and infrasound stimuli. *PLoS ONE*, *15*(2), e0229088. https://doi.org/10.1371/journal.pone.0229088

Beugels, J., van den Hurk, J., Peters, J. C., Heuts, E. M., Tuinder, S. M. H., Goebel, R., & van der Hulst, R. R. W. J. (2020). Somatotopic mapping of the human breast using 7 T functional MRI. *NeuroImage*, *204*, 116201. https://doi.org/10.1016/j.neuroimage.2019.116201

- Boslaugh, S., & Watters, P. A. (2008). *Statistics in a Nutshell: A Desktop Quick Reference*. O'Reilly Media. https://books.google.com/books/about/Statistics in a Nutshell.html?id=ZnhgO65Pyl4C
- Burton, H., Agato, A., & Sinclair, R. J. (2012). Repetition learning of vibrotactile temporal sequences: An fMRI study in blind and sighted individuals. *Brain Research*, *1433*, 69–79. https://doi.org/10.1016/j.brainres.2011.11.039
- Burton, H., Sinclair, R. J., & McLaren, D. G. (2008). Cortical network for vibrotactile attention: a fMRI study. *Human Brain Mapping*, 29(2), 207–221. https://doi.org/10.1002/hbm.20384
- Cassady, K., Ruitenberg, M. F. L., Reuter-Lorenz, P. A., Tommerdahl, M., & Seidler, R. D. (2020). Neural Dedifferentiation across the Lifespan in the Motor and Somatosensory Systems. *Cerebral Cortex*, *30*(6), 3704–3716. https://doi.org/10.1093/cercor/bhz336
- Cerliani, L., Mennes, M., Thomas, R. M., Di Martino, A., Thioux, M., & Keysers, C. (2015). Increased functional connectivity between subcortical and cortical resting-state networks in Autism spectrum disorder. *JAMA Psychiatry*, 72(8), 767–777. https://doi.org/10.1001/jamapsychiatry.2015.0101
- Chakravarty, M. M., Rosa-Neto, P., Broadbent, S., Evans, A. C., & Collins, D. L. (2009). Robust S1, S2, and thalamic activations in individual subjects with vibrotactile stimulation at 1.5 and 3.0 T. *Human Brain Mapping*, 30(4), 1328–1337. https://doi.org/10.1002/hbm.20598
- Choi, M. H., Kim, S. P., Kim, H. S., & Chung, S. C. (2016). Inter-and Intradigit Somatotopic Map of High-Frequency Vibration Stimulations in Human Primary Somatosensory Cortex. *Medicine (United States)*, *95*(20), 1–9. https://doi.org/10.1097/MD.0000000000003714
- Chung, Y. G., Kim, J., Han, S. W., Kim, H. S., Choi, M. H., Chung, S. C., Park, J. Y., & Kim, S. P. (2013). Frequency-dependent patterns of somatosensory cortical responses to vibrotactile stimulation in humans: A fMRI study. *Brain Research*, *1504*, 47–57. https://doi.org/10.1016/j.brainres.2013.02.003
- Cole, D. M., Stämpfli, P., Gandia, R., Schibli, L., Gantner, S., Schuetz, P., & Meier, M. L. (2022). In the back of your mind: Cortical mapping of tactile and proprioceptive paraspinal afferent inputs. *Human Brain Mapping*. 43(16), 4943–4953. https://doi.org/10.1002/hbm.26052
- Corbetta, M., Burton, H., Sinclair, R. J., Conturo, T. E., Akbudak, E., & McDonald, J. W. (2002). Functional sreorganisation and stability of somatosensory-motor cortical topography in a tetraplegic subject with late recovery. *Proceedings of the National Academy of Sciences of the United States of America*, *99*(26), 17066–17071. https://doi.org/10.1073/pnas.262669099
- Deuchert, M., Ruben, J., Schwiemann, J., Meyer, R., Thees, S., Krause, T., Blankenburg, F., Villringer, K., Kurth, R., Curio, G., & Villringer, A. (2002). Event-related fMRI of the somatosensory system using electrical finger stimulation. *NeuroReport*, *13*(3), 365–369. https://doi.org/10.1097/00001756-200203040-00023
- Ding, H., Ming, D., Wan, B., Li, Q., Qin, W., & Yu, C. (2016). Enhanced spontaneous functional connectivity of the superior temporal gyrus in early deafness. *Scientific Reports*, 6, 23239. https://doi.org/10.1038/srep23239
- Du, Y., & Fan, Y. (2013). Group information guided ICA for fMRI data analysis. *NeuroImage*, *69*, 157–197. https://doi.org/10.1016/j.neuroimage.2012.11.008
- Du, Y., Fu, Z., Sui, J., Gao, S., Xing, Y., Lin, D., Salman, M., Abrol, A., Rahaman, M. A., Chen, J., Hong, L. E., Kochunov, P., Osuch, E. A., & Calhoun, V. D. (2020). NeuroMark: An automated and adaptive ICA based pipeline to identify reproducible fMRI markers of brain disorders. *NeuroImage: Clinical*, *28*, 102375. https://doi.org/10.1016/j.nicl.2020.102375
- Du, Y., He, X., & Calhoun, V. D. (2021). SMART (splitting-merging assisted reliable) Independent Component Analysis for Brain Functional Networks. *2021 43rd Annual International Conference of the IEEE Engineering in Medicine & Biology Society (EMBC)*, 3263–3266. https://doi.org/10.1109/EMBC46164.2021.9630284
- Eickhoff, S. B., & Müller, V. I. (2015). Functional Connectivity. In *Brain Mapping: An Encyclopedic Reference*, *2,* 187–201. https://doi.org/10.1016/B978-0-12-397025-1.00212-8
- Elseoud, A. A., Littow, H., Remes, J., Starck, T., Nikkinen, J., Nissilä, J., Timonen, M., Tervonen, O., & Kiviniemi, V. (2011). Group-ICA model order highlights patterns of functional brain connectivity. *Frontiers in Systems Neuroscience*, *5*, 37. https://doi.org/10.3389/fnsys.2011.00037
- Francis, S. T., Kelly, E. F., Bowtell, R., Dunseath, W. J. R., Folger, S. E., & McGlone, F. (2000). fMRI of the responses to vibratory stimulation of digit tips. *NeuroImage*, *11*(3), 188–202. https://doi.org/10.1006/nimg.2000.0541
- Friedrich, J., Mückschel, M., & Beste, C. (2018). Specific properties of the SI and SII somatosensory areas and their effects on motor control: a system neurophysiological study. *Brain Structure and Function*, *223*(2), 687–699. https://doi.org/10.1007/s00429-017-1515-y

- Golaszewski, S. M., Siedentopf, C. M., Baldauf, E., Koppelstaetter, F., Eisner, W., Unterrainer, J., Guendisch, G. M., Mottaghy, F. M., & Felber, S. R. (2002). Functional magnetic resonance imaging of the human sensorimoto cortex using a novel vibrotactile stimulator. *NeuroImage*, *17*(1), 421–430. https://doi.org/10.1006/nimg.2002.1195
- Golaszewski, S. M., Siedentopf, C. M., Koppelstaetter, F., Fend, M., Ischebeck, A., Gonzalez-Felipe, V., Haala, I., Struhal, W., Mottaghy, F. M., Gallasch, E., Felber, S. R., & Gerstenbrand, F. (2006). Human brain structures related to plantar vibrotactile stimulation: A functional magnetic resonance imaging study. *NeuroImage*, 29(3), 923–929. https://doi.org/10.1016/j.neuroimage.2005.08.052
- Goltz, D., Pleger, B., Thiel, S., Villringer, A., & Müller, M. M. (2013). Sustained spatial attention to vibrotactile stimulation in the flutter range: Relevant brain regions and their interaction. *PLoS ONE*, 8(12), 1–12. https://doi.org/10.1371/journal.pone.0084196
- Hagen, M. C., & Pardo, J. V. (2002). PET studies of somatosensory processing of light touch. *Behavioural Brain Research*, 135(1-2), 133–140. https://doi.org/10.1016/s0166-4328(02)00142-0
- Hegner, Y. L., Lee, Y., Grodd, W., & Braun, C. (2010). Comparing Tactile Pattern and Vibrotactile Frequency Discrimination: A Human fMRI Study. *Journal of Neurophysiology*, *103*(6), 3115–3122. https://doi.org/10.1152/jn.00940.2009
- Hegner, Y. L., Saur, R., Veit, R., Butts, R., Leiberg, S., Grodd, W., & Braun, C. (2007). BOLD adaptation in vibrotactile stimulation: Neuronal networks involved in frequency discrimination. *Journal of Neurophysiology*, *97*(1), 264–271. https://doi.org/10.1152/jn.00617.2006
- Iandolo, R., Bellini, A., Saiote, C., Marre, I., Bommarito, G., Oesingmann, N., Fleysher, L., Mancardi, G. L., Casadio, M., & Inglese, M. (2018). Neural correlates of lower limbs proprioception: An fMRI study of foot position matching. *Human Brain Mapping*, *39*(5), 1929–1944. https://doi.org/10.1002/hbm.23972
- Jaatela, J., Aydogan, D. B., Nurmi, T., Vallinoja, J., & Piitulainen, H. (2022). Identification of Proprioceptive Thalamocortical Tracts in Children: Comparison of fMRI, MEG, and Manual Seeding of Probabilistic Tractography. *Cerebral Cortex*, 32(17), 37366–3751. https://doi.org/10.1093/cercor/bhab444
- Jung, W. M., Ryu, Y., Park, H. J., Lee, H., & Chae, Y. (2018). Brain activation during the expectations of sensory experience for cutaneous electrical stimulation. *NeuroImage: Clinical*, *19*, 982–989. https://doi.org/10.1016/j.nicl.2018.06.022
- Kim, J., Chung, Y. G., Chung, S. C., Bulthoff, H. H., & Kim, S. P. (2016). Neural sCategorisation of Vibrotactile Frequency in Flutter and Vibration Stimulations: An fMRI Study. *IEEE Transactions on Haptics*, *9*(4), 455–464. https://doi.org/10.1109/TOH.2016.2593727
- Kim, J., Müller, K.-R., Chung, Y. G., Chung, S.-C., Park, J.-Y., Bülthoff, H. H., & Kim, S.-P. (2015). Distributed functions of detection and discrimination of vibrotactile stimuli in the hierarchical human somatosensory system. *Frontiers in Human Neuroscience*, 8(January), 1–10. https://doi.org/10.3389/fnhum.2014.01070
- Maldjian, J. A., Laurienti, P. J., Kraft, R. A., & Burdette, J. H. (2003). An automated method for neuroanatomic and cytoarchitectonic atlas-based interrogation of fMRI data sets. *NeuroImage*, *19*(3), 1233–1239. https://doi.org/10.1016/S1053-8119(03)00169-1
- Malone, P. S., Eberhardt, S. P., Wimmer, K., Sprouse, C., Klein, R., Glomb, K., Scholl, C. A., Bokeria, L., Cho, P., Deco, G., Jiang, X., Bernstein, L. E., & Riesenhuber, M. (2019). Neural mechanisms of vibrotactile categorisation. *Human Brain Mapping*, 40(10), 3078–3090. https://doi.org/10.1002/hbm.24581
- Moritz, C. H., Haughton, V. M., Cordes, D., Quigley, M., & Meyerand, M. E. (2000). Whole-brain Functional MR Imaging Activation from a Finger-tapping Task Examined with Independent Component Analysis. *American Journal of Neuroradiology*, *21*(9), 1629–1635.
- Motovilova, E., & Winkler, S. A. (2022). Overview of Methods for Noise and Heat Reduction in MRI Gradient Coils. *Frontiers in Physics*, *10*, 907619. https://doi.org/10.3389/fphy.2022.907619
- Nazarian, B., Caron-Guyon, J., Anton, J. L., Sein, J., Baurberg, J., Catz, N., & Kavounoudias, A. (2022). A new patterned air-flow device to reveal the network for tactile motion coding using fMRI. *Journal of Neuroscience Methods*, *365*, 109397. https://doi.org/https://doi.org/10.1016/j.jneumeth.2021.109397
- Oldfield, R. C. (1971). The assessment and analysis of handedness: The Edinburgh inventory. *Neuropsychologia*, 9(1), 97–113. https://doi.org/10.1016/0028-3932(71)90067-4
- Park, J. W., Kim, Y. H., Jang, S. H., Chang, W. H., Park, C. H., & Kim, S. T. (2010). Dynamic changes in the corticosubcortical network during early motor learning. *NeuroRehabilitation*, *26*(2), 95–103. https://doi.org/10.3233/NRE-2010-0540

- Pechenkova, E. V., Nosikova, I. N., Rumshiskaya, A. D., Litvinova, L. D., Rukavishnikov, I. V., Mershina, E. A., Sinitsin, V. E., Van Ombergen, A., Jeurissen, B., Jillings, S. D., Laureys, S., Sijbers, J., Grishin, A., Chernikova, L. A., Naumov, I. A., Kornilova, L. N., Wuyts, F. L., Tomilovskaya, E. S., & Kozlovskaya, I. B. (2019). Alterations of functional brain connectivity after long-duration spaceflight as revealed by fMRI. *Frontiers in Physiology*, 10(May), 761. https://doi.org/10.3389/fphys.2019.00761
- Pfannmöller, J. P., Greiner, M., Balasubramanian, M., & Lotze, M. (2016). High-resolution fMRI investigations of the fingertip somatotopy and variability in BA3b and BA1 of the primary somatosensory cortex.

 Neuroscience, 339, 667–677. https://doi.org/10.1016/j.neuroscience.2016.10.036
- Puckett, A. M., Bollmann, S., Barth, M., & Cunnington, R. (2017). Measuring the effects of attention to individual fingertips in somatosensory cortex using ultra-high field (7T) fMRI. *NeuroImage*, *161*, 179–187. https://doi.org/10.1016/j.neuroimage.2017.08.014
- Quintana, D. S. (2023). A guide for calculating study-level statistical power for meta-analyses. *Advances in Methods and Practices in Psychological Science*, *6*,(1). https://doi.org/10.1177/25152459221147260
- Rabe, F., Kikkert, S., & Wenderoth, N. (2021). Finger representations in primary somatosensory cortex are modulated by a vibrotactile working memory task. *BioRxiv*, *340*(1), 1–33. https://doi.org/10.1101/2021.10.29.466459
- Renier, L. A., Anurova, I., De Volder, A. G., Carlson, S., VanMeter, J., & Rauschecker, J. P. (2009). Multisensory Integration of Sounds and Vibrotactile Stimuli in Processing Streams for "What" and "Where." *Journal of Neuroscience*, 29(35), 10950–10960. https://doi.org/10.1523/JNEUROSCI.0910-09.2009
- Rondinoni, C., Amaro, E., Cendes, F., dos Santos, A. C., & Salmon, C. E. G. (2013). Effect of scanner acoustic background noise on strict resting-state fMRI. *Brazilian Journal of Medical and Biological Research*, 46(4), 359–367. https://doi.org/10.1590/1414-431X20132799
- Rosazza, C., Minati, M., Ghielmetti, F., Mandelli, M. L., & Bruzzone, M. G. (2012). Functional connectivity during resting-state functional MR imaging: Study of the correspondence between independent component analysis and region-of-interest Based methods. *American Journal of Neuroradiology*, *33*(1), 180–187. https://doi.org/10.3174/ajnr.A2733
- Sauvage, C., Poirriez, S., Manto, M., Jissendi, P., & Habas, C. (2011). Reevaluating brain networks activated during mental imagery of finger movements using probabilistic Tensorial Independent Component Analysis (TICA). *Brain Imaging and Behavior*, 5(2), 137–148. https://doi.org/10.1007/s11682-011-9118-3
- Schweisfurth, M. A., Frahm, J., & Schweizer, R. (2014). Individual fMRI maps of all phalanges and digit bases of all fingers in human primary somatosensory cortex. *Frontiers in Human Neuroscience*, 8(SEP), 1–14. https://doi.org/10.3389/fnhum.2014.00658
- Schweisfurth, M. A., Frahm, J., & Schweizer, R. (2015). Individual left-hand and right-hand intra-digit representations in human primary somatosensory cortex. *European Journal of Neuroscience*, 42(5), 2155–2163. https://doi.org/10.1111/ejn.12978
- Schweisfurth, M. A., Schweizer, R., & Frahm, J. (2011). Functional MRI indicates consistent intra-digit topographic maps in the little but not the index finger within the human primary somatosensory cortex. *NeuroImage*, 56(4), 2138–2143. https://doi.org/10.1016/j.neuroimage.2011.03.038
- Sengupta, A., Ackerley, R., Watkins, R. H., Panchuelo, R. S., Paul, G., Wessberg, J., & Francis, S. (2019). Global responses to microstimulation at 7T and comparison with vibrotactile stimulation. *Proceedings of Joint Annual Meeting ISMRM-ESMRMB*, 0149. https://archive.ismrm.org/2018/0149.html
- Seri, F. A. S., Abd Hamid, A. I., Abdullah, J. M., Idris, Z., & Omar, H. (2019). Brain responses to frequency changes due to vibratory stimulation of human fingertips: An fMRI study. *Journal of Physics: Conference Series*, 1248(1), 1–6. https://doi.org/10.1088/1742-6596/1248/1/012029
- Seri, F. A. S., Abd Hamid, A. I., Abdullah, J. M., Idris, Z., & Omar, H. (2020). Brain responses to high frequencies (270 Hz-480 Hz) changes due to vibratory stimulation of human fingertips: An fMRI study. *Journal of Physics: Conference Series*, 1497, 012012. https://doi.org/10.1088/1742-6596/1497/1/012012
- Siedentopf, C. M., Heubach, K., Ischebeck, A., Gallasch, E., Fend, M., Mottaghy, F. M., Koppelstaetter, F., Haala, I. A., Krause, B. J., Felber, S., Gerstenbrand, F., & Golaszewski, S. M. (2008). Variability of BOLD response evoked by foot vibrotactile stimulation: Influence of vibration amplitude and stimulus waveform.

 NeuroImage, 41(2), 504–510. https://doi.org/10.1016/j.neuroimage.2008.02.049
- Sormaz, M., Murphy, C., Wang, H. T., Hymers, M., Karapanagiotidis, T., Poerio, G., Margulies, D. S., Jefferies, E., & Smallwood, J. (2018). Default mode network can support the level of detail in experience during active task

- states. *Proceedings of the National Academy of Sciences of the United States of America*, 115(37), 9318–9323. https://doi.org/10.1073/pnas.1721259115
- Sörös, P., Marmurek, J., Tam, F., Baker, N., Staines, W. R., & Graham, S. J. (2007). Functional MRI of working memory and selective attention in vibrotactile frequency discrimination. *BMC Neuroscience*, 8, 1–10. https://doi.org/10.1186/1471-2202-8-48
- Sung, E. J., Yoo, S. S., Yoon, H. W., Oh, S. S., Han, Y., & Park, H. W. (2007). Brain activation related to affective dimension during thermal stimulation in humans: A functional magnetic resonance imaging study. *International Journal of Neuroscience*, 117(7), 1011–1027. https://doi.org/10.1080/00207450600934432
- Tomasi, D., & Volkow, N. D. (2011). Association between functional connectivity hubs and brain networks. *Cerebral Cortex*, 21(9), 2003–2013. https://doi.org/10.1093/cercor/bhq268
- Uluç, I., Schmidt, T. T., Wu, Y. hao, & Blankenburg, F. (2018). Content-specific codes of parametric auditory working memory in humans. *NeuroImage*, 183, 254–262. https://doi.org/10.1016/j.neuroimage.2018.08.024
- Willoughby, W. R., Thoenes, K., & Bolding, M. (2021). Somatotopic Arrangement of the Human Primary Somatosensory Cortex Derived From Functional Magnetic Resonance Imaging. *Frontiers in Neuroscience*, *14*, 598482. https://doi.org/10.3389/fnins.2020.598482
- Woolgar, A., & Zopf, R. (2017). Multisensory coding in the multiple-demand regions: vibrotactile task information is coded in frontoparietal cortex. *Journal of Neurophysiology*, *118*, 703–716. https://doi.org/10.1152/jn.00559.2016
- World Medical Association. (2013). World Medical Association declaration of Helsinki: Ethical principles for medical research involving human subjects. *JAMA*, *310*(20), 2191–2194. https://doi.org/10.1001/jama.2013.281053
- Wu, L., Caprihan, A., Bustillo, J., Mayer, A., & Calhoun, V. (2018). An approach to directly link ICA and seed-based functional connectivity: Application to schizophrenia. *NeuroImage*, *179*, 448–470. https://doi.org/10.1016/j.neuroimage.2018.06.024
- Wu, Y., Velenosi, L. A., & Blankenburg, F. (2021). Response modality-dependent categorical choice representations for vibrotactile comparisons. *NeuroImage*, *226*, 117592. https://doi.org/10.1016/j.neuroimage.2020.117592
- Xu, J., Potenza, M. N., & Calhoun, V. D. (2013). Spatial ICA reveals functional activity hidden from traditional fMRI GLM-based analyses. *Frontiers in Neuroscience*, 7, 154. https://doi.org/10.3389/fnins.2013.00154
- Zhao, W., Li, H., Hu, G., Hao, Y., Zhang, Q., Wu, J., Frederick, B. B., & Cong, F. (2021). Consistency of independent component analysis for FMRI. *Journal of Neuroscience Methods*, *351*, 109013. https://doi.org/10.1016/j.jneumeth.2020.109013